

# GLASS MELTING AND ITS INNOVATION POTENTIALS: BUBBLE REMOVAL UNDER THE EFFECT OF THE CENTRIFUGAL FORCE

LUBOMÍR NĚMEC, VLADISLAVA TONAROVÁ

*Laboratory of Inorganic Materials*

*Joint Workplace of the Institute of Inorganic Chemistry AS CR, v.v.i. and the Institute of Chemical Technology Prague, Technická 5, 166 28 Prague, Czech Republic*

E-mail: Lubomir.Nemec@vscht.cz

Submitted June 6, 2008; accepted September 19, 2008

**Keywords:** Glass melt, Bubble removal, Centrifugal force, Modelling, Rotating cylinder

*The fining process may be enhanced by an additional force on bubbles in the glass melt. This study deals with the behaviour of a single bubble in the glass melt by a centrifugal force obtained in a rotating discontinuous cylinder. A model for bubble movement and size changes (growth or dissolution) for a single bubble in a glass melt exposed the combined gravitational and centrifugal fields has been developed and calculations of the bubble behaviour in a glass melt contained in a vertical rotating cylinder have been performed for a TV panel glass. The crucial factor of the removal of a bubble from the melt appeared to be its partial or complete dissolution in the molten glass, governed by the number of different gas species present, their concentrations in the bubble, as well as by their physical or chemical solubility and diffusion coefficients in the molten glass. The results of the calculations have shown that the bubble-separation (removal by moving the bubble to the glass melt surface) mechanism should be preferred to dissolution. The recommended bubble removal/separation conditions can be derived from the general found dependencies between the bubble-removal times and the cylinder-rotation velocity for different glass types, temperatures and cylinder dimensions. The minimum separation time, dependent on the applied temperature, rotation rate, filling level, size of cylinder, will direct to the most effective bubble separation conditions and appears to be a guide for practical applications. The position of the minimum in the curve of separation time versus cylinder rotation velocity and these bubble-separation times depend on the temperature, external pressure, the initial actual bubble radius (bubble radius changes if the rotational velocity is changed) and composition of the bubble, composition of the molten glass (gas properties in the given glass), the cylinder radius and the degree to which the cylinder is filled with glass.*

## INTRODUCTION

A substantial acceleration of the process homogenising (and especially the removal of gas bubbles and seeds) of the glass melt will result in a decrease in the energy consumption and ensures the high melting performance of glass-melting furnaces or facilitates their miniaturisation. The bubble-removal process (fining) is one of the crucial processes in glass production. In the course of fining, bubbles should be effectively removed from the melt. This can be accomplished by either dissolution or separation (removal) of the rising and growing bubbles from the melt by the buoyancy force. Some possibilities to improve the separation (here is meant not dissolution of bubbles but removal) of the bubbles from the melt include the common use of refining agents, the saturation of the glass by rapidly diffusing gasses [1], the application of reduced pressure [2-5], and the application of external forces such as supersonic waves [6], surface force [7-8] and centrifugal force [9-13]. When a rotating cylinder in vertical

position, fed with molten glass, (see the schematic Figure 1) is applied for fining, the rapid removal of the bubbles having diameters between  $3 \times 10^{-5} - 8 \times 10^{-4}$  m from a continuous rotating cylinder is claimed. However, no exact knowledge exists about behaviour of single bubbles in the centrifugal field under different fining conditions. The aim of this work is the detailed examination of single-bubble behaviour by a modelling approach (the experimental laboratory investigations are also prepared) by the influence of the centrifugal force in a rotating cylinder, working in discontinuous regime and filled with molten glass, and to find optimum process parameters (rotation speed, size, temperature, filling by the molten glass) suitable for industrial application.

A model describing the behaviour of a single bubble (movements, growth or shrinkage) in a molten glass under the influence of centrifugal forces has been designed [14]. The very first calculations indicated a significant influence of the cylinder size [15], temperature and rotation velocity [16]. An increase in efficiency

*Paper presented at the seminar "Advanced Glass Materials and Innovative Glass Melting Technology in the Year 2020", Brig, Switzerland, March 26-29, 2008.*

seemed to have been obtained through the partial filling of the cylinder, which confirmed the results of previous calculations where it was shown that the centrifuging efficiency on fining of the melt in the partially filled cylinder will be increased when the cylinder radius is increased and when the thickness of glass layer inside the cylinder becomes thinner [15].

The complex study being presented deals with the effect of temperature, pressure, the bubble's initial composition, cylinder-rotation velocity, cylinder radius and the degree to which the cylinder is filled with the melt on the bubble-removal process in the cylinder. The mechanisms of complete dissolution of the bubble or its separation (removal) by centrifuging are discussed and the general conditions for the bubble removal in the centrifugal field are derived from the results of the modelling studies.

### THEORETICAL

In the gravitational field and quiescent glass melt, the bubble rises to the glass level. Gases will diffuse in or out of the bubble depending on the gas-concentration gradient on the bubble surface. When the centrifugal force is applied,

- a) the pressure inside the bubble considerably increases (especially at the cylinder wall), and
- b) the bubble starts to move from the wall in the direction of the rotation centre.

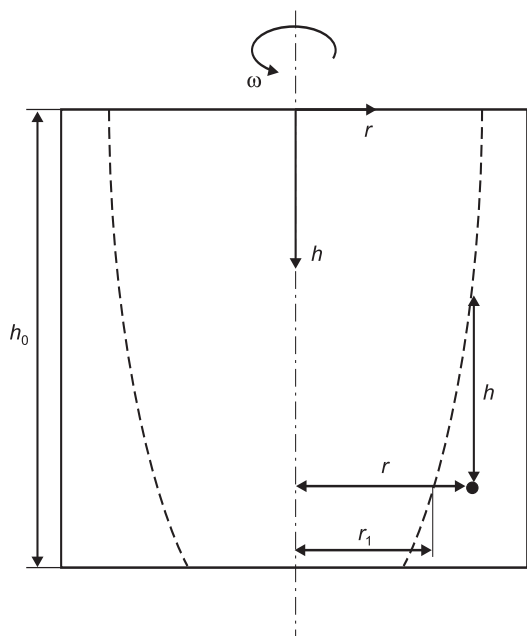


Figure 1. The schematic representation of the rotating cylinder with the bubble position in the melt.

As a consequence of this increase in pressure, the bubble having the initial radius  $a_0$  (at given temperature and normal pressure) tends to shrink and the bubble motion towards the cylinder centre decelerates. The bubble shrinkage is caused not only by gas contraction but also by the potential diffusion of the gases in the melt. The bubble behaviour is thus dependent also on the conditions of the diffusion process, such as temperature, the diffusion coefficient of the gas in question in the molten glass (only temperature dependence of the diffusion coefficients is considered), the total gas concentration in the melt as well as the initial bubble composition. The decreasing pressure during the bubble's drifting towards the cylinder axis supports the bubble's growth but the effect of the centrifugal force on bubble centrifuging decreases. The separation or removal efficiency of the bubble by the centrifugal force is hence generally determined by two counteracting effects: the local pressures inside the bubble will increase and will lead to bubble shrinkage and in some cases complete dissolution and, the local centrifugal acceleration will lead to fast movements of the bubble (with lower density) relative to the glass melt to the glass melt-furnace atmosphere interface. The shrinkage of the bubbles will counteract the removal of bubbles by the separation process. Both effects (shrinkage or dissolution and bubble movement) also increase with the cylinder-rotation velocity.

We have created a model that describes the bubble behaviour (change of radius and movement in the melt) in the melt inside a rotating cylinder. This model is described in detail in [14]. At isothermal conditions, the radius change of the bubble in the rotating cylinder is given by the equation

$$\frac{da}{d\tau} = \frac{1}{p_{tot}} \left[ \frac{2\rho^2 a^3}{27\eta} (g^2 + \omega^4 r^2) + RT \sum_{i=1}^n \frac{k_i}{M_i} (c_{ib} - c_{ia}) \right]$$

$$p_{tot} = \left( p_{ex} + \rho gh + 4\sigma / 3a + \frac{\rho\omega^2 (r^2 - r_1^2)}{2} \right) \quad (1a,b)$$

whereas for the pressure of the  $i$ -th gas inside the bubble, it holds that

$$\frac{dp_i}{d\tau} = \frac{3RT}{M_i a} k_i (c_{ib} - c_{ia}) - \frac{3p_i}{a} \frac{da}{d\tau} \quad (2)$$

where  $a$  is the bubble radius,  $\tau$  is time,  $\rho$  and  $\eta$  are the glass density and viscosity,  $p_{ex}$  is the external pressure,  $h'$  is the depth of the bubble below the glass level,  $\sigma$  is the surface tension of the glass,  $\omega$  is the angular rotation velocity of the cylinder [radials/s],  $r$  is the bubble distance from the centre axis of the cylinder,  $k_i$  is the mass-transfer coefficient of the  $i$ -th gas,  $c_{ib}$  and  $c_{ia}$  are respectively the bulk and bubble surface concentrations of the  $i$ -th gas dissolved in the glass melt ( $c_{ib}$  is consi-

dered constant with time),  $r_1(h)$  is the variable radial coordinate of the curved glass level in the depth  $h$  below the cylinder top (with the cylinder being only partially filled with glass).

#### Calculation Conditions

The glass for TV panels was used as the model glass, because the diffusion and solubility data of the individual gases were available from recent measurements. The glass and gas properties necessary to model the bubble behaviour are summarised in [16]. The following parameters have been applied:

$t = 1300, 1400$  and  $1500^\circ\text{C}$ ,  $p_{ex} = 0.1, 0.25, 0.5$  and  $1$  bar,  $\omega \in \langle 10; 400 \text{ s}^{-1} \rangle$ ,  $a_0 = 5 \times 10^{-5}, 1 \times 10^{-4}, 3 \times 10^{-4}, 4 \times 10^{-4}, 5 \times 10^{-4}$  and  $6 \times 10^{-4}$  m,  $r_0, R_0 = 0.04, 0.25$  and  $0.5$  m,  $V/V_0 = 0.25, 0.5, 0.75$  and  $0.95$ ,  $h_0 = 0.5$  m.

In the calculation,  $t$  is temperature,  $a_0$  is the initial bubble radius,  $r_0$  is the initial radial position of the bubble,  $R_0$  is the cylinder radius,  $V_0$  and  $V$  are the cylinder volume and the volume of the glass melt in the cylinder and  $h_0$  is the height of the rotating cylinder.

The assumed initial gas content of the bubbles corresponds to the bubble composition in these melts under certain conditions and at constant temperature after some time elapses and the bubble size and composition remaining almost constant as long as the conditions are also constant. The initial stationary bubble compositions at temperatures of  $1300\text{-}1500^\circ\text{C}$  and a pressure of 1bar in the TV glass fined by antimony oxide (case I) or without any fining agent and dissolved water (case II) are given in Table 1.

Table 1. The initial bubble stationary composition at temperatures  $1300\text{-}1500^\circ\text{C}$  and pressure 1 bar in the TV glass refined by antimony oxide (case I) and in the glass without any refining agent, melted from dry raw materials (case II).

| case I  | gas (vol. %)    |                |       |                |                  |
|---------|-----------------|----------------|-------|----------------|------------------|
|         | CO <sub>2</sub> | N <sub>2</sub> | Ar    | O <sub>2</sub> | H <sub>2</sub> O |
| 1300°C  | 23.6            | 23.2           | 0.073 | 28.3           | 24.9             |
| 1400°C  | 4.0             | 3.2            | 0.009 | 66.7           | 26.1             |
| 1500°C  | 2.0             | 1.5            | 0.004 | 69.4           | 27.0             |
| case II | gas (vol. %)    |                |       |                |                  |
|         | CO <sub>2</sub> | N <sub>2</sub> | Ar    | O <sub>2</sub> | H <sub>2</sub> O |
| 1300°C  | 26.0            | 71.0           | 0.69  | 2.3            | 0                |
| 1400°C  | 37.9            | 51.8           | 0.71  | 9.7            | 0                |
| 1500°C  | 49.9            | 32.3           | 0.69  | 17.1           | 0                |

## RESULTS OF BUBBLE MODELLING

Due to the effect of pressure on the gas transport between the bubbles and the melt, two mechanisms of bubble removal are possible, both can take place at certain conditions as it has been confirmed by our modelling: bubble centrifuging (separation and bubble removal) towards the cylinder centre and complete bubble dissolution in the molten glass. As may be assumed, only small bubbles at high rotation velocities and starting from positions characterised by a great radial distance may be completely dissolved in the melt. Recent modelling results have also indicated that the initial composition of bubbles and temperature dependent solubility of gases in the melt play a significant role in the prime mechanism of bubble removal and, consequently, in the bubble-removal times [15]. Generally, those bubbles containing a well soluble gas with a high diffusion coefficient and low bulk concentration in the melt dissolve easily (especially at high local pressures). The concentration of chemically soluble gases in glass melts depends on the temperature and glass composition (the concentration of fining agents, for example); subsequently, the mechanism of bubble removal by centrifuging also depends on the mentioned parameters. Therefore, such bubbles that contain fining gas, like the above-mentioned oxygen in our case, easily dissolve in glass at low temperatures but mostly grow or only slowly dissolve at high temperatures. The bubbles containing gases, that are only hardly soluble in the melt, e.g. nitrogen, dissolve only slowly at higher rotation velocities. The multicomponent bubbles generally exhibit a low tendency to dissolve completely as the concentrations of the individual gases on the bubble boundary are proportional to the gas content in the bubble. Table 2 below is useful for a preliminary comparison of the roles of dissolution and separation mechanisms of various types of bubbles. The table provides the number of bubbles, which showed the maximum removal/dissolution times at the given temperature (regardless of the cylinder rotation velocity) and with the given initial bubble composition. The value attained for the bubble which began at the cylinder bottom and near the cylinder circumference is hereinafter covered by the term 'maximum bubble-removal time',  $\tau_{\max}$ . Three categories of these mechanisms have been distinguished: the complete bubble dissolution, the removal of almost dissolved bubbles by separation and the separation of insoluble bubbles to the cylinder centre. The first two categories indicate dissolution as a controlling mechanism. The results in Table 2 suggest that the complete and almost complete dissolution (43 bubbles) were most frequently the slowest mechanisms with respect to the centrifuging of undissolved bubbles (17 bubbles). The value of the actual maximum

bubble-removal time (determined below) by the mechanism of complete bubble dissolution relates however to defined bubble initial radius (which will be determined later in this work for some cases) and should in fact be higher than has been calculated here for bubbles of a selected initial size. Therefore, the separation of bubbles by centrifuging ought to be intuitively preferred to the complete bubble dissolution mechanism.

The following figures present the dependences between the maximum bubble-removal times (both by separation from the melt and complete dissolution) and the cylinder-angular velocities for bubbles starting from the bottom part and the wall (circumference) of the cylinder under various temperatures, pressures, initial glass compositions, cylinder radii and for different degrees to which the cylinder is filled with glass. The complete bubble dissolution is always designated by an asterisk (the actual maximum values are higher, as will be shown later). The example of results involving the maximum bubble-removal times as a function of the cylinder-angular velocity for the whole range of multi-component bubble sizes and for case I (bubbles in glass with a fining agent, see Table 1) and for a temperature of 1400°C are shown in Figure 2. As shown by this figure, minima and maxima of  $\tau_{max}$  versus cylinder angular velocity occur on the curves for the two smallest bubbles sizes. The same dependence of the maximum bubble-removal times,  $\tau_{max}$ , for the smallest bubbles having an initial radius of  $5 \times 10^{-5}$  m and for temperatures of 1300-1500°C is depicted in Figure 3. The apparent small shifts of the minima to larger  $\omega$ -values at increasing temperature will be discussed later. The typical changes of bubble composition and radius after the

pressure due rotation set in the cylinder and during centrifuging are presented in Figures 4a,b. The initial decrease in the concentrations of the gases dissolved in the melt (oxygen, water vapour, carbon dioxide) is caused by their diffusion out of the bubble (as arises from Figure 4a) and accompanied by a small decrease in the bubble size (as can be seen in Figure 4b). However, the rapid decrease of pressure inside the bubble during centrifuging, as the bubble moves to the cylinder centre axis, causes the backward diffusion of gases into the bubble while the bubble radius grows, due to both the pressure release and gas diffusion. The character of bubble behaviour is thus influenced by the process conditions, leading sometimes to complete bubble dissolution in the glass. The impact of the various external pressures on the dependence between the maximum bubble-removal time and the cylinder-angle velocity for very small bubbles with  $a_0 = 5 \times 10^{-5}$  m is clear from Figure 5.

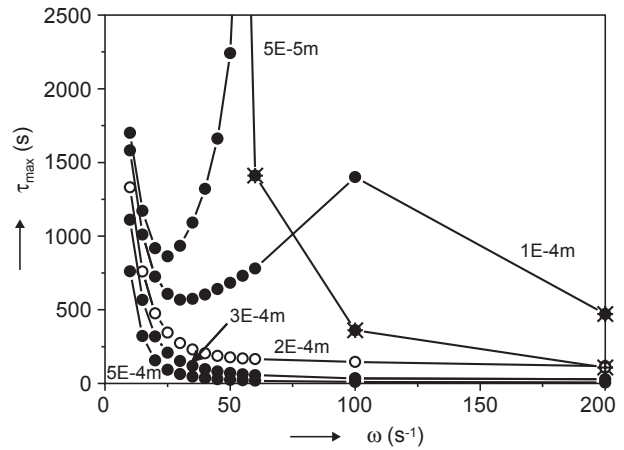


Figure 2. The dependence between  $\tau_{max}$  and the cylinder angular velocity  $\omega$  (0-200  $s^{-1}$ ) at 1400°C,  $p_{ex} = 1$  bar, case I,  $a_0 = 5 \times 10^{-5}$ ;  $1 \times 10^{-4}$ ;  $2 \times 10^{-4}$ ;  $3 \times 10^{-4}$ ;  $5 \times 10^{-4}$  m,  $R_0 = 0.25$  m,  $V/V_0 = 0.5$ . Asterisks mark the bubble complete dissolution.

Table 2. The numbers of the bubbles showing the maximum bubble-removal times according to their removal mechanism,  $p_{ex} = 1$  bar,  $R_0 = 0.25$  m,  $V/V_0 = 0.5$ , all calculated rotation velocities of the cylinder involved.

| Number of bubbles showing the maximum bubble-removal times (longest lasting bubbles) |                             |                                   |                  |
|--|-----------------------------|-----------------------------------|------------------|
| initial bubble composition   | completely dissolved bubble | almost dissolved separated bubble | separated bubble |
| oxygen, 1300°C   | 2                           | 3                                 | 0                |
| oxygen, 1400°C   | 3                           | 1                                 | 1                |
| oxygen, 1500°C   | 1                           | 2                                 | 2                |
| CO <sub>2</sub> , 1300°C   | 5                           | 0                                 | 0                |
| CO <sub>2</sub> , 1400°C   | 3                           | 1                                 | 1                |
| CO <sub>2</sub> , 1500°C   | 5                           | 0                                 | 0                |
| N <sub>2</sub> , 1300°C  | 2                           | 1                                 | 2                |
| N <sub>2</sub> , 1400°C  | 3                           | 2                                 | 0                |
| N <sub>2</sub> , 1500°C  | 5                           | 0                                 | 0                |
| case I, 1300°C   | 2                           | 0                                 | 3                |
| case I, 1400°C   | 1                           | 0                                 | 4                |
| case I, 1500°C   | 1                           | 0                                 | 4                |
| total  | 33                          | 10                                | 17               |

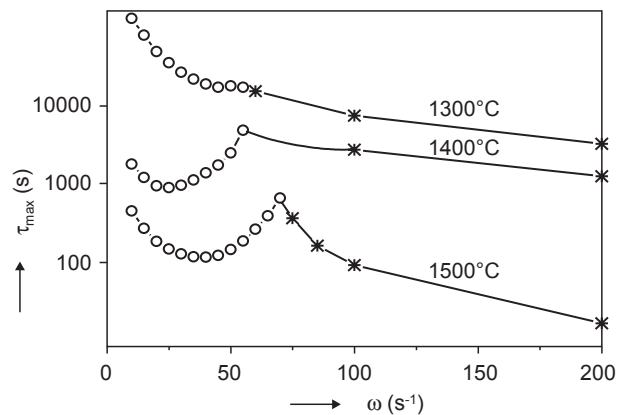


Figure 3. The dependence between  $\tau_{max}$  and the cylinder angular velocity  $\omega$  (0-200  $s^{-1}$ ) at 1300, 1400 and 1500°C,  $p_{ex} = 1$  bar,  $a_0 = 5 \times 10^{-5}$ ,  $R_0 = 0.25$  m,  $V/V_0 = 0.5$ . Asterisks mark the bubble complete dissolution. Effect of temperature.

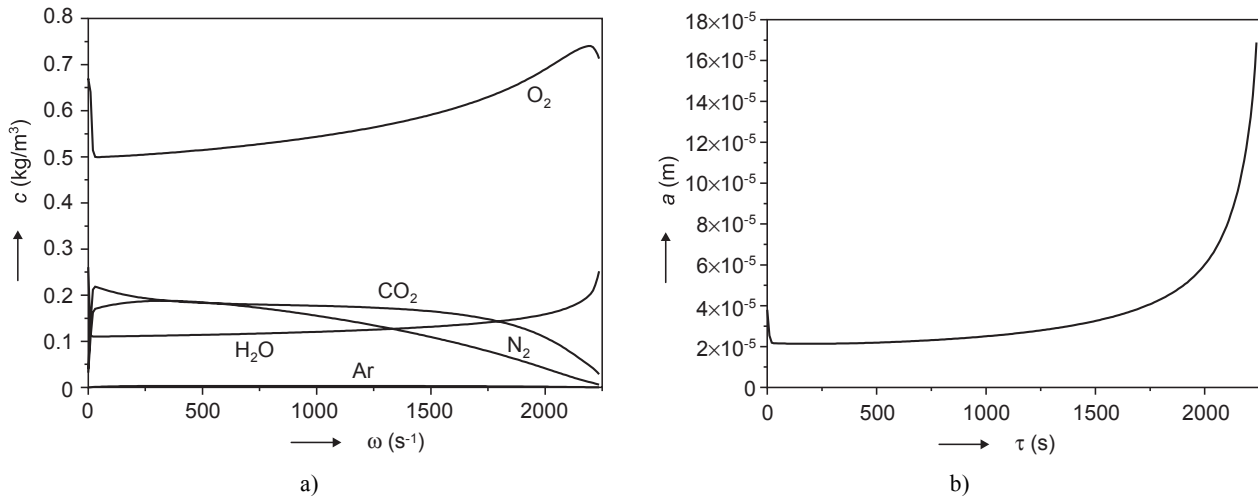


Figure 4. The dependence of volume concentrations of the gases in the bubble and of the bubble radius on time;  $t = 1400^\circ\text{C}$ ,  $p_{ex} = 1$  bar, case I,  $a_0 = 5 \times 10^{-5}$  m (at given temperature and pressure 1 bar),  $\omega = 50$  s<sup>-1</sup>,  $R_0 = 0.25$  m,  $V/V_0 = 0.5$  (the total pressure sets in the cylinder at  $\tau = 0$ ).

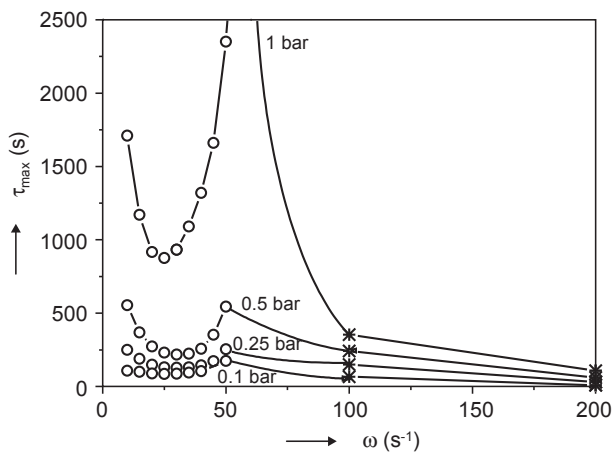


Figure 5. The dependence between  $\tau_{max}$  and the cylinder angular velocity  $\omega$  (0-200 s<sup>-1</sup>) at  $1400^\circ\text{C}$ ,  $p_{ex} = 0.1, 0.25, 0.5$  and 1 bar,  $a_0 = 5 \times 10^{-5}$ ,  $R_0 = 0.25$  m,  $V/V_0 = 0.5$ . Asterisks mark the bubble complete dissolution. Effect of external pressure.

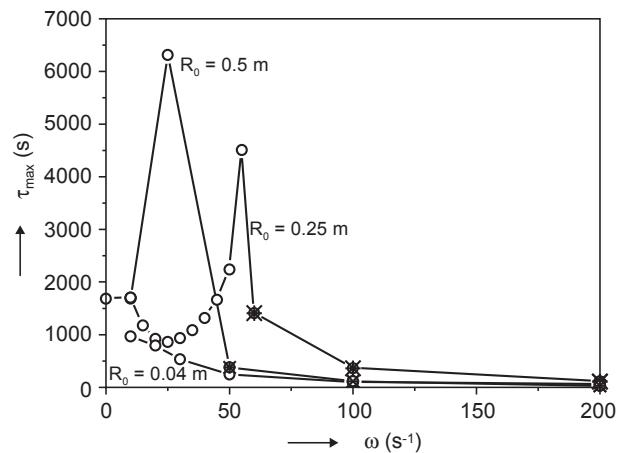


Figure 6. The dependence between  $\tau_{max}$  and the cylinder angular velocity  $\omega$  (0-200 s<sup>-1</sup>) at  $1400^\circ\text{C}$ ,  $p_{ex} = 1$  bar,  $a_0 = 5 \times 10^{-5}$ ,  $R_0 = 0.04, 0.25$  and 0.5 m,  $V/V_0 = 0.5$ . Asterisks mark the bubble complete dissolution. Effect of cylinder radius.

Also a distinct decrease in  $\tau_{max}$  with pressure can be observed; the minimum remains in approximately the same position. An alternative bubble composition is obtained if the fining agent is absent from the glass and dry raw materials are used for melting. Bubbles contain mainly carbon dioxide and nitrogen, the second of which is hardly soluble in oxidized glass melts. It may therefore be expected that gas diffusion out of the bubbles would be suppressed, which would also hold true for bubble dissolution. The results for the mentioned initial bubble composition (case II) at  $1300^\circ\text{C}$  and in the broad region of cylinder angular velocities showed the first minimum for a bubble with an initial radius of  $5 \times 10^{-5}$  m only at about  $\omega = 300$  s<sup>-1</sup>. The question of

proper cylinder size may be solved by further modelling results. The results of the bubble modelling at a temperature of  $1400^\circ\text{C}$ ,  $p_{ex} = 1$  bar and cylinder radius 0.5 m have shown, that the position of the minima for small bubbles was shifted towards distinctly lower angular velocities with respect to the values presented in Figure 2. The dependence of the maximum bubble-removal time for the bubbles of  $a_0 = 5 \times 10^{-5}$  m on  $\omega$  and on the three cylinder radii (with the cylinder radius 0.04 m being intended for the laboratory verification of the results) is then depicted in Figure 6. The substantial impact of the cylinder radius on bubble-removal times and on the position, as well as the existence of the minima in the curves showing  $\tau_{max}$  versus  $\omega$ , is evident. Our

earlier results have already shown the significance of the degree to which the cylinder has been filled with the melt for bubble removal [15,16]. Figure 7 provides the standard dependence between  $\tau_{\max}$  and the cylinder angular velocity for the various initial bubble sizes at 1400°C,  $p_{ex} = 1$  bar and for a low filling level of the cylinder with glass, equivalent to  $V/V_0 = 0.25$ . The lower values of  $\tau_{\max}$  and the shift of the minima to higher-angle velocities are evident when Figure 7 is compared to Figure 2. The overall dependence between  $\tau_{\max}$  at various degrees to which the cylinder is filled with glass and the cylinder-angle velocity for the bubbles with  $a_0 = 5 \times 10^{-5}$  m is then depicted in Figure 8. The shift of the minimum to higher cylinder-angle velocities is apparent as the volume of glass in the cylinder decreases.

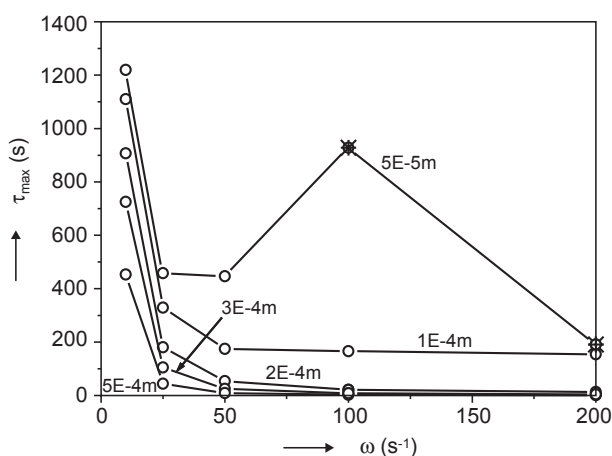


Figure 7. The dependence between  $\tau_{\max}$  and the cylinder angular velocity  $\omega$  (0-200  $s^{-1}$ ) at 1400°C,  $p_{ex} = 1$  bar, case I,  $a_0 = 5 \times 10^{-5}$ ,  $1 \times 10^{-4}$ ,  $2 \times 10^{-4}$ ,  $3 \times 10^{-4}$ ,  $5 \times 10^{-4}$ ,  $R_0 = 0.25$ ,  $V/V_0 = 0.25$ . Asterisks mark the bubble complete dissolution.

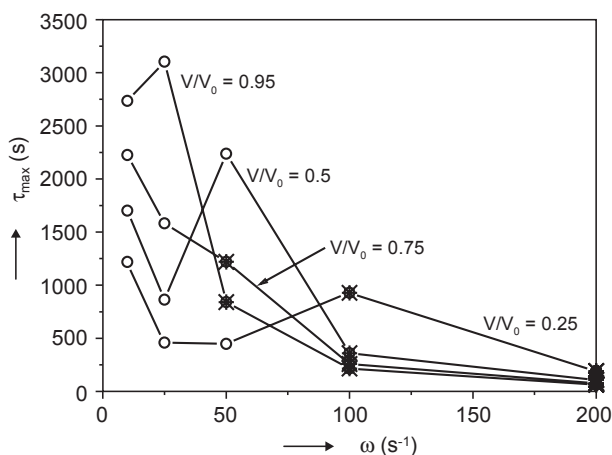


Figure 8. The dependence between  $\tau_{\max}$  and the cylinder angular velocity  $\omega$  (0-200  $s^{-1}$ ) at 1400°C. Asterisks mark the bubble complete dissolution. Effect of cylinder filling by glass.

The presented results show the rather complicated behaviour of bubbles in the rotating cylinder, which can make it difficult to determine the optimal fining conditions for this centrifugal system. It is therefore necessary to understand the general features of the process.

## DISCUSSION

Prior to a discussion of the diverse results of bubble modelling, the main principles of the general behaviour of a bubble in the viscous glass and in the combined gravitational and centrifugal field should be presented along with the significant factors restricting its applications. The behaviour of the bubble is principally determined by gas compressibility and the direction and intensity of the gas diffusion between the bubbles and the glass melt, which in particular distinguishes the behaviour of solid or liquid particles from that of bubbles in the centrifugal field. Generally it may be stated that conditions supporting gas diffusion from the melt into the bubbles (melt supersaturation by gases with respect to the bubbles) and large initial radii of the bubbles are in favour of the mechanism of the bubble centrifuging and shift the position of the observed minimum of the bubble-removal time to higher cylinder angular velocities, i.e. the higher rotation velocities may be used for effective centrifuging. The opposite conditions (low glass saturation by gases and small bubbles) lead to the complete dissolution of rather small bubbles. The mentioned tendencies help to explain the general shape of the curve showing the dependence between the bubble-removal time and the cylinder angular velocity, as is schematically presented in Figure 9. Bubbles at low rotational velocities are mostly removed by the combined effect of the gravitational and centrifugal

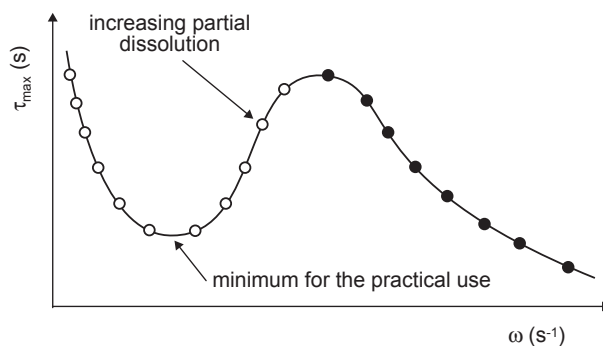


Figure 9. The shape of the general dependence between the bubble-removal time,  $\tau_F$ , in the rotating cylinder with glass melt and the cylinder angular velocity. ○ - centrifuging, ● - complete dissolution.

field, and the proportional effect of the centrifugal field increases with the rotational velocity while the bubble-removal times decrease. Bubbles dissolve only during their initial residence period and later grow (see Figure 3b). Once the minimum bubble-removal time is attained, the gas diffusion out of bubbles begins to play a more important role because of the increasing pressure, the bubbles partially dissolve and the bubble-removal times grow. In its maximum, the bubble-removal time indicates an already completely dissolved bubble. At higher cylinder-rotation velocities, bubbles completely dissolve in the glass and the bubble-dissolution times decrease with the cylinder-rotation velocity due to the growing pressure inside the bubbles. The minimum in the graph at relatively low rotational speeds seems to often be convenient for practical applications, as will be discussed later.

The problematic factors inhibiting the potential application of centrifugal fining may be classified as follows:

1. A disadvantageous bubble-removal mechanism. The complete bubble dissolution appears to be too slow and technically problematic. Both problems will be discussed in the section dealing with dissolution.
2. Too high absolute values of the bubble-removal times or too high relative bubble-removal times (The relative bubble removal time is the ratio between the bubble-removal time attained by centrifuging and the time the bubble needs to pass through the glass layer of the same thickness as is exhibited by the layer in the non-rotating cylinder.).
3. Too high temperatures, which may overheat the cylinder.
4. Too high pressures, which may mechanically destabilise the cylinder.
5. Too small bubbles entering the cylinder, which are very slowly separated by centrifuging.
6. Too small fining performance, resulting from an unsuitable cylinder size or content of glass.

It seems useful to discuss the impact of all of the fining parameters with respect to the mentioned restricting factors.

The position of the minimum  
in the graph of  $\tau_{\max}$  versus  $\omega$

*The impact of temperature and initial bubble composition:* If the glass contains a fining agent, the melt is super-saturated by the fining gas at higher temperatures, and the minimum is shifted to higher cylinder angular velocities (from about 25 s<sup>-1</sup> at 1400°C to about 45 s<sup>-1</sup> at 1500°C for the bubble  $a_0 = 5 \times 10^{-5}$  m). At low temperatures around 1300°C, the bubble  $a_0 = 5 \times 10^{-5}$  m partially

dissolves because of a low saturation of the glass by the gases, but the low values of the diffusion coefficients make the dissolution considerably slow and the dissolving bubble is finally removed by centrifuging even at 50 s<sup>-1</sup>. The minimum of the bubble removal time and the bubble-dissolution region at 1300°C are located at higher  $\omega$ ; the position of the minimum for the bubble  $a_0 = 5 \times 10^{-5}$  m is around  $\omega = 55$  s<sup>-1</sup> (see Figure 3).

If no fining agents are added to the batch and dried raw materials are used, the bubbles contain nearly exclusively carbon dioxide and nitrogen. The low number of the components and low saturation of the glass by the gases enhance the bubble dissolution, as a result of which the minimum for bubble separation time should occur at low cylinder angular velocities. This is especially true at temperatures of 1400 and 1500°C, where the bubbles dissolve already at  $\omega = 10$  s<sup>-1</sup> and the minimum theoretically would be below this value. At 1300°C, the very slow bubble dissolution shifts the minimum for bubble separation time to high cylinder-rotation velocities, with the position of the minimum for the bubble with  $a_0 = 5 \times 10^{-5}$  m at 1300°C being at about 300 s<sup>-1</sup>. A comparison of  $\tau_{\max}$  at two temperatures, involving the dissolution area at 1400°C and the position of the minimum at 1300°C, is presented in Figure 10.

*The impact of pressure:* If the total pressure in the bubbles is not too high (with an angular velocity lower than about 50 s<sup>-1</sup> in the cylinder  $R_0 = 0.25$  m and  $V/V_0 = 0.5$ ), the low external pressure reduces bubble dissolution and shifts the position of the minimum to higher cylinder-angle velocities. The effect of pressure is only negligible, as can be seen in Figure 5, probably due to the already existing chemical super-saturation of the glass by the fining gas.

*The impact of the initial bubble size:* The bubble-dissolution time significantly increases with the bubble size, which is why the position of the minimum and the region of the bubble dissolution shift to a considerably higher  $\omega$  with growing  $a_0$  (see Figure 2). While the minimum for  $a_0 = 5 \times 10^{-5}$  is at 25 s<sup>-1</sup>, its position shifts to approximately 30 s<sup>-1</sup> for  $a_0 = 1 \times 10^{-4}$  m and is between  $\omega = 100$  s<sup>-1</sup> and 200 s<sup>-1</sup> for  $a_0 = 2 \times 10^{-4}$  m.

*The impact of the cylinder radius and the degree to which the cylinder is filled with glass:* As  $R_0$  and  $V/V_0$  increases, so does the total pressure inside of the bubbles, and the tendency to bubble dissolution is enhanced. The minimum for bubble separation time shifts to lower cylinder-angle velocities. The impact of the cylinder radius is shown in Figure 6, where the position of the minimum for  $R_0 = 0.04$  m is at  $\omega > 50$  s<sup>-1</sup>, for  $R_0 = 0.25$  m it is at 25 s<sup>-1</sup> and for  $R_0 = 0.5$  m it would lie below  $\omega = 10$  s<sup>-1</sup>. Figure 8 demonstrates the shift of the minimum for bubble separation time from  $\omega = 50$  s<sup>-1</sup> at  $V/V_0 = 0.25$  to  $\omega < 10$  s<sup>-1</sup> at  $V/V_0 = 0.95$ .

The role of the dissolution mechanism

Table 2 indicates that the mechanism of complete dissolution should be slow. Here we provide a more detailed evaluation. The values of  $\tau_{\max}$  corresponding to the dissolved bubbles presented in Table 2 did not represent the actual maximum bubble-dissolution times. The maximum bubble-dissolution time in the cylinder,  $\tau_{\text{dissmax}} = \tau_{\max}$ , can be clarified by the following image: imagine a bubble starting from a position close to the shell of the rotating cylinder. If the effect of gravitation is neglected, the bubble moves radially to the central axis of the cylinder. The element of its radial movement may be expressed as

$$dr = \frac{2\rho\omega^2ra^2}{9\eta} d\tau \quad (3)$$

Complete dissolution is a complex process, depending on both physical and chemical parameters. If the glass is supersaturated by gases under normal pressure (the case of glass melt with a fining agent at higher temperatures), the bubble can not be dissolved close to the glass level unless it is extremely small. The role of the surface forces then becomes important and the bubble completely dissolves owing to the high value of the pressure term,  $2\sigma/a$ . Despite the bubble's complex behaviour in the rotating melt (pressure changes, e.g.), the modelling results admitted sometimes to describe the bubble complete dissolution by a linear dependence between bubble radius and time. This assumption is especially satisfactory for the dissolution of bubbles in the glass without a fining agent

$$a = a_0 - k\tau \quad (4)$$

where  $a_0$  is the initial bubble radius at the given total pressure and  $k$  (m/s) is the constant rate of bubble dissolution in the rotating cylinder. A substitution of Equation (4) into (3) and an integration yields

$$\ln \frac{R_0}{r_i} = \frac{2\rho\omega^2}{9\eta} \left( a_0^2\tau_{\text{diss}} - a_0k\tau_{\text{diss}}^2 + \frac{k^2\tau_{\text{diss}}^3}{3} \right) \quad (5)$$

where  $r_i$  is now the constant average value of the layer of glass melt in the rotating cylinder and  $\tau_{\text{diss}}$  is the bubble-dissolution time. If the bubble dissolves just at the glass level, the value of  $\tau_{\text{diss}}$  is  $a_0/k$ , after a substitution of which into (5) we obtain

$$\tau_{\text{diss}} = \frac{27\eta \ln \frac{R_0}{r_i}}{2\rho\omega^2 a_0^2} \quad (6)$$

If the initial bubble is smaller than  $a_0$ , it will dissolve before reaching the glass-atmosphere interface and its dissolution time will be lower than the value of  $\tau_{\text{diss}}$  from Equation (6). If, on the other hand, the initial

bubble is greater than  $a_0$ , its radial velocity will be higher than in the case described by Equation (6), the bubble will reach the glass level and its separation time will also be less than in the case described by Equation (6). A bubble dissolving right at the glass level thus exhibits the maximum removal time,  $\tau_{\text{dissmax}}(r_0)$ , of all the bubbles originating at the given starting position.

When the starting position of the bubble is shifted towards the cylinder's centre, the value of the maximum bubble-dissolution (and in the same time segregation) time decreases and attains a zero value at  $r_0 = r_1$ . The dissolving bubble starting close to the cylinder shell and subsequently dissolved just at the curved glass level therefore exhibits the maximum dissolution time of all the dissolved bubbles

$$\tau_{\text{dissmax}}(R_0) = \tau_{\max} \quad (7)$$

Based on Equations (6) and (7), the value of the maximum bubble-removal time for the dissolution mechanism may be modelled in terms of the maximum bubble-removal time of bubbles of different initial sizes, starting from a position close to the cylinder shell, an example of which is provided in Figure 11, where the values of  $\tau_{\max}$  have been calculated for bubbles dissolving in the glass with a fining agent at 1400°C,  $p_{\text{ex}} = 1$  bar and at angular velocities of 100 and 200 s<sup>-1</sup>. Earlier results have shown that the bubble  $a_0 = 5 \times 10^{-5}$  m at 100 s<sup>-1</sup> and the bubble  $a_0 = 1 \times 10^{-4}$  m at 200 s<sup>-1</sup> completely dissolved in glass. The largest dissolved bubble at  $\omega = 100$  s<sup>-1</sup> had a radius of  $9.5 \times 10^{-5}$  m and  $\tau_{\max} = 2579$  s, the largest dissolved bubble at 200 s<sup>-1</sup> exhibited  $a_0 = 1.25 \times 10^{-4}$  m and  $\tau_{\max} = 1206$  s. The maximum in the curve of the bubble-removal times versus initial bubble radius is very sharp.

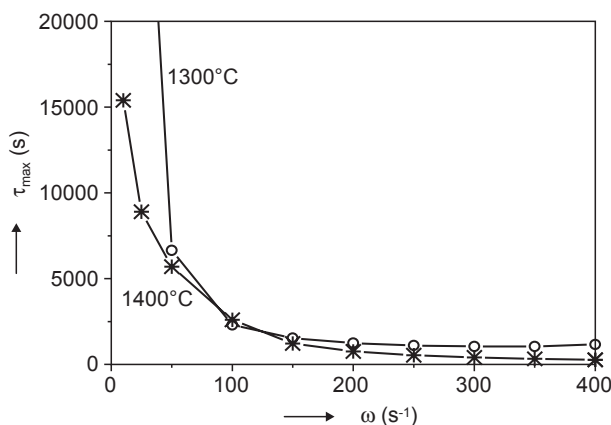


Figure 10. The dependence between  $\tau_{\max}$  and the cylinder angular velocity  $\omega$  (0-400 s<sup>-1</sup>),  $t = 1300$  and  $1400^\circ\text{C}$ ,  $p_{\text{ex}} = 1$  bar, case II,  $a_0 = 5 \times 10^{-5}$ ,  $R_0 = 0.25$ ,  $V/V_0 = 0.5$ . Asterisks mark the bubble complete dissolution. The local pressure at the bottom and circumference of the cylinder is given as a function of  $\omega$  in Figure 12.

Thus, the possibility presents itself that complete bubble dissolution may become a beneficial bubble-removal mechanism at high cylinder-rotation velocities, where the bubble-dissolution times should be low (see Figure 9). When searching for a proper example, the bubble removal (by dissolution) from the glass without any fining agent at temperatures of 1400 and 1500°C appears convenient. The values of  $\tau_{\max}$  have therefore been calculated by applying the here presented bubble model (Equations (1-2)) and also by using Equation (6). The values of  $a_0$  in Equation (6) corresponded to the bubble initial radii at given temperature and total pressure at the circumference of the rotating cylinder. Figure 12 presents both sets of  $\tau_{\max}$  values for a temperature of 1400°C while Figure 13 the same values for 1500°C. The values of  $\tau_{\max}$  calculated for the glass with fining agents under the same conditions and of the total pressure close to the cylinder shell have also been added in the figures. In order to enable a comparison of the dissolution mechanism with the mechanism of free bubble rising by the gravitational force, the time of bubble rising ( $a_0 = 5 \times 10^{-5}$  m) through the layer of glass having the same thickness as the layer in the rotating cylinder has been included.

The  $\tau_{\max}$  values according to Equation (6) are slightly higher than in the case of the bubble model, but any  $\tau_{\max}$  values at lower and medium angle velocities are too high for effective fining. At 1400°C, the dissolution by centrifuging starts to compete with the bubble free rising only from about  $\omega > 200$  s<sup>-1</sup>, whereas at 1500°C from about  $\omega > 250$  s<sup>-1</sup>. Nevertheless, the high pressures around 15 bar (at 1400°C) and 25 bar (at 1500°C) at the cylinder shell at the rotation rates represent a serious

obstacle for such an application. At 1300°C, bubbles in the glass without any fining agent do not dissolve before  $\omega = 400$  s<sup>-1</sup>, the dissolving bubbles in the glass with a fining agent exhibit  $\tau_{\max} = 6850$  s at  $\omega = 100$  s<sup>-1</sup> and  $\tau_{\max} = 3050$  s at  $\omega = 200$  s<sup>-1</sup>, i.e. values also too high for effective bubble removal.

When the data on the bubble dissolution are summarised, the mechanism appears disadvantageous. The maximum bubble-dissolution times (represented by  $\tau_{\max}$ ) are always too high at lower rotational veloci-

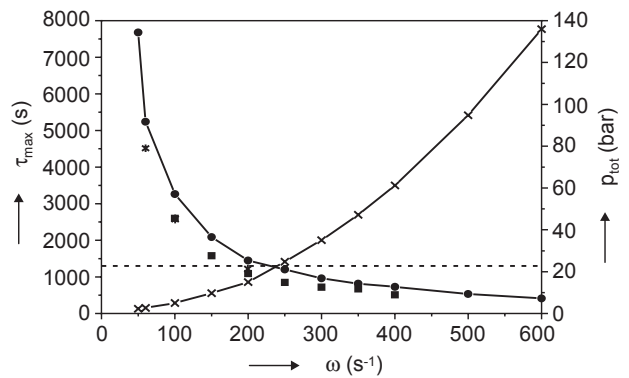


Figure 12. The dependence between the dissolution time of the largest dissolved bubble and  $\omega$  (50-600 s<sup>-1</sup>),  $t = 1400^\circ\text{C}$ ,  $p_{\text{ex}} = 1$  bar, case II,  $R_0 = 0.25$  m,  $V/V_0 = 0.5$ . ● -  $\tau_{\max}$  (Equation (6)), ■ - numerically calculated by using the here presented bubble model (Equations (1-2)), case II; \* - numerically calculated by using the bubble model (case I), ---- the bubble-removal time by bubble rising for the glass layer of a thickness of 0.074 m,  $a_0 = 5 \times 10^{-5}$  m, × -  $p_{\text{tot}}$  at the bottom and circumference of the cylinder.

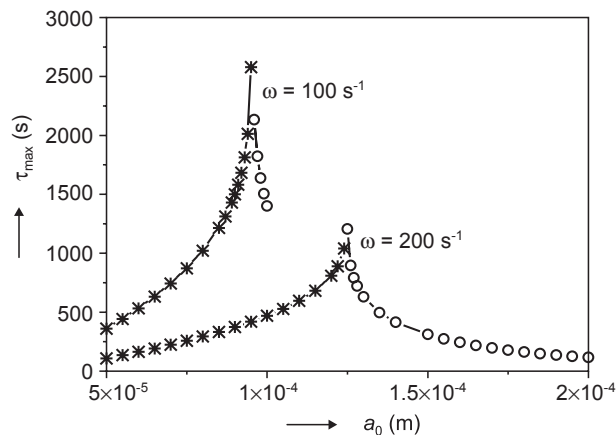


Figure 11. The dependence between the bubble-removal time and the initial bubble radius ( $a_0$  at given temperature and pressure 1 bar). The bubble starting at the bottom and circumference of the cylinder, case I,  $t = 1400^\circ\text{C}$ ,  $p_{\text{ex}} = 1$  bar,  $\omega = 100$  and  $200$  s<sup>-1</sup>,  $V/V_0 = 0.5$ . Asterisks mark the bubble complete dissolution. The radius of the maximal dissolved bubble at  $\omega = 100$  s<sup>-1</sup> was  $9.5 \times 10^{-5}$  m, at  $\omega = 200$  s<sup>-1</sup> was  $1.25 \times 10^{-4}$  m.

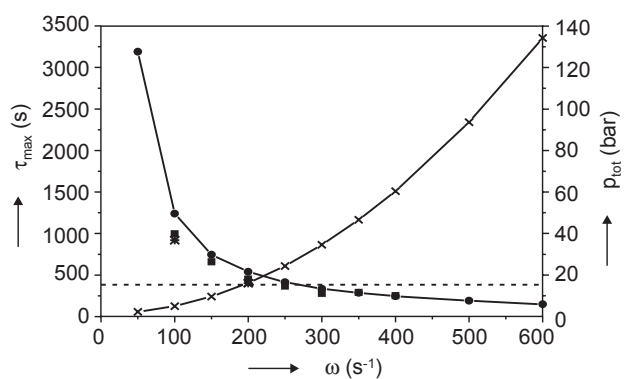


Figure 13. The dependence between the dissolution time of the largest dissolved bubble and  $\omega$  (100-600 s<sup>-1</sup>),  $t = 1500^\circ\text{C}$ ,  $p_{\text{ex}} = 1$  bar, case II,  $R_0 = 0.25$  m,  $V/V_0 = 0.5$ . ● -  $\tau_{\max}$  (Equation (6)), ■ - numerically calculated by using the here presented bubble model (Equations (1-2)), case II; \* - numerically calculated by using the bubble model (case I), ---- the bubble-removal time by bubble rising for the glass layer of a thickness of 0.074 m,  $a_0 = 5 \times 10^{-5}$  m, × -  $p_{\text{tot}}$  at the bottom and circumference of the cylinder.

ties and cannot compete with free bubble rising by the gravitational force. The low bubble-dissolution times at higher rotational velocities are accompanied by pressures on the cylinder shell that are too high. High pressures at high temperatures cause serious technical problems. It is therefore advisable to avoid the bubble-dissolution mechanism when selecting proper fining conditions.

The impact of initial bubble composition

Two initial bubble compositions have been investigated in this work because of their practical importance, namely bubbles coming from the glass with a fining agent (case I) and bubbles in the glass without any fining agent, potentially melted from dried raw materials (case II). Both stationary bubble compositions are provided in Table 1. Similar features are typical for bubbles in other glass type. The previous section argues to avoid the use of the bubble-dissolution mechanism, in which the initial bubble composition plays a significant role. Following the results in the previous section, the bubbles of the initial composition corresponding to case II should be avoided by using the fining agent and temperatures of 1400 and 1500°C. The bubbles of case I exhibit complete dissolution above  $\omega = 100 \text{ s}^{-1}$  at all examined temperatures, the interval at  $\omega > 100 \text{ s}^{-1}$  should be therefore excluded too. As a result of this restriction, the bubbles of case I should be removed by separation only at low cylinder-rotation velocities and at all examined temperatures whereas bubbles of case II do not dissolve throughout the examined range of rotational velocities only at low temperature 1300°C (see Figure 10). The minima of  $\tau_{\text{max}}$  as a function of  $\omega$  for bubbles of case I have already been presented in Figures 2, 3 and 5-8. The use of cylinder-angle velocities, corresponding to a minimum  $\tau_{\text{max}}$ , offers a suitable condition for centrifugal fining. The restricting factors of the application will be discussed in the following paragraphs of this section.

The bubbles of case II did not dissolve at 1300°C even at high angular velocity 400  $\text{s}^{-1}$  due to very slow diffusion of the  $\text{CO}_2$  and  $\text{N}_2$  gas out of bubbles whereas

bubble of case I dissolved easier at the same temperature because they contain some fining gas, quickly soluble in the melt (see Table 1). An opportunity arises to apply low angular velocities  $\omega < 100 \text{ s}^{-1}$  (too high pressure sets at the cylinder circumference at  $\omega > 100 \text{ s}^{-1}$ , see Figures 12, 13) and low temperatures around 1300°C for the bubbles of case II. In order to evaluate benefit of the mentioned conditions, the obtained values of  $\tau_{\text{max}}$  were compared with the values of the times which the smallest bubble needs to rise freely through the glass layer of the same thickness as is created in the cylinder ( $\omega = 0$ ). The values of  $\tau_{\text{max}}$  for the cylinder angle velocities up to  $\omega = 200 \text{ s}^{-1}$ , for bubbles of case II and at a temperature of 1300°C as a function of  $a_0$  are presented in Figure 14. The bubble centrifuging times,  $\tau_{\text{max}}$ , are much lower than the bubble rising times ( $\omega = 0$ ), particularly at  $\omega > 50 \text{ s}^{-1}$ , but high values of  $\tau_{\text{max}}$  are seen for small bubbles. Table 3 shows that the  $\tau_{\text{max}}$  values for bubbles of case II are lower than those of the bubbles of case I; nevertheless, the maximum bubble-removal times for  $a_0 = 5 \times 10^{-5} \text{ m}$  are high for both the bubble compositions and glasses (case I and II). This is particularly dangerous when centrifuging glass without any fining agent (with multicomponent II). Such glass usually contains some tiny bubbles before centrifuging.

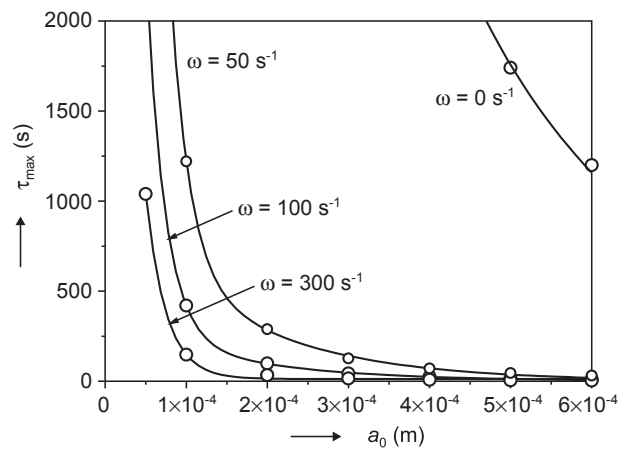


Figure 14. The dependence between  $\tau_{\text{max}}$  and  $a_0$ ,  $t = 1300^\circ\text{C}$ ,  $p_{\text{ex}} = 1 \text{ bar}$ , case II,  $\omega = 0, 50, 100$  and  $300 \text{ s}^{-1}$ ,  $R_0 = 0.25 \text{ m}$ ,  $V/V_0 = 0.5$ . All bubbles removed by separation.

Table 3. The dependence between  $\tau_{\text{max}}$  and  $a_0$ ,  $t = 1300^\circ\text{C}$ ,  $p_{\text{ex}} = 1 \text{ bar}$ , case I and II,  $\omega = 25, 50$  and  $100 \text{ s}^{-1}$ ,  $R_0 = 0.25 \text{ m}$ ,  $V/V_0 = 0.5$ .

| $a_0$ (m)          | $\omega = 25 \text{ s}^{-1}$ |                    | $\omega = 50 \text{ s}^{-1}$ |         | $\omega = 100 \text{ s}^{-1}$ |         |
|--------------------|------------------------------|--------------------|------------------------------|---------|-------------------------------|---------|
|                    | case I                       | case II            | case I                       | case II | case I                        | case II |
| $5 \times 10^{-5}$ | 31100                        | 35500 <sup>x</sup> | 16000                        | 6650    | 4350 <sup>x</sup>             | 2300    |
| $1 \times 10^{-4}$ | 6430                         | 5450               | 1710                         | 1220    | 707                           | 420     |
| $2 \times 10^{-4}$ | 1470                         | 1290               | 366                          | 289     | 141                           | 98.5    |
| $3 \times 10^{-4}$ | 636                          | 566                | 152                          | 127     | 56.6                          | 43.2    |
| $4 \times 10^{-4}$ | 349                          | 317                | 81.5                         | 71.2    | 29.7                          | 24.2    |
| $5 \times 10^{-4}$ | 218                          | 202                | 50.8                         | 45.5    | 18.4                          | 15.4    |
| $6 \times 10^{-4}$ | 150                          | 140                | 34.8                         | 31.5    | 12.5                          | 10.7    |

<sup>x</sup> bubble dissolved

Both the initial bubble compositions and glass compositions, obtainable after the melting process of these batches, thus have their own regions of beneficial conditions. The lower temperatures around 1300°C and cylinder-angle velocities below 50-100 s<sup>-1</sup> are suitable for glasses without any fining agents (producing bubbles of the composition of case II); however, practical application should be preceded by laboratory melts to examine the occurrence of very small bubbles. At higher temperatures, i.e. of 1400-1500°C, glass with a fining agent has to be applied, producing bubbles of case I, and optimal cylinder-angle velocities ranging between 25-40 s<sup>-1</sup>. The highest fining temperatures need to solve some technical problems, especially the way of melt heating in the rotating cylinder.

The impact of temperature

The main interest will be aimed at the bubbles of the case I composition because the bubbles of the case II may be efficiently removed only at lower temperatures. Figures 15-17 provide information on the behaviour of case I bubbles at temperatures of 1300-1500°C in the form of  $\tau_{max}$  versus  $a_0$  dependences. To compare the centrifuging mechanism with the bubble-rising mechanism due to gravitation, the removal times of the smallest bubble of  $a_0 = 5 \times 10^{-5}$  m rising freely through the layer of glass having the same thickness as the layer in the cylinder ( $\omega = 0$  s<sup>-1</sup>) is also plotted in the following Figures 15-17.

The values of  $\tau_{max}$  at 1300°C are below  $\omega = 0$  s<sup>-1</sup> for  $\omega > 10$  s<sup>-1</sup>, whereas the best values are at  $\omega = 25$ -50 s<sup>-1</sup>, and at  $\omega \geq 100$  s<sup>-1</sup> dissolution occurs. The  $\tau_{max}$  values for  $a_0 < 1 \times 10^{-5}$  m are relatively high because of the high glass viscosity. At 1400 and 1500°C, super-saturation by the fining gas in the glass melt hinders the bubble dissolution and low glass viscosity accelerates the bubble separation by centrifuging. The values of  $\tau_{max}$  at 1400°C and  $\omega = 100$  s<sup>-1</sup> in Figure 16 are too high for bubbles with  $a_0 \leq 1 \times 10^{-4}$  m (existence of a maximum in  $\tau_{max}$  versus  $a_0$ ). The high-angle velocity may be applied only when the small bubbles can be removed by their having grown without rotation, otherwise the  $\omega = 25$  s<sup>-1</sup> represents the optimal angle velocity at the given temperature. It is analogous for temperatures of 1500°C in Figure 17, where the optimal cylinder-angle velocity occurs around  $\omega = 40$  s<sup>-1</sup>.

When trying to evaluate the relative efficiency of centrifuging, the ratio between the average value of the maximum bubble-removal times obtained by centrifuging and the average value of bubble-removal time acquired by rising is useful,  $\tau_{max}(\omega)/\bar{\tau}(\omega = 0)$ . The average values have been calculated involving the bubbles with  $a_0$  in the range of 2-6  $\times 10^{-4}$  m (smaller bubbles are not involved as they may dissolve and deform the average value). The low value of the ratio

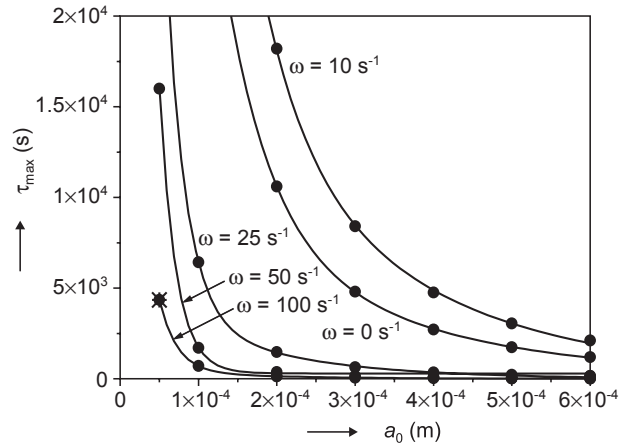


Figure 15. The dependence between  $\tau_{max}$  and  $a_0$ ,  $t = 1300^\circ\text{C}$ ,  $p_{ex} = 1$  bar, case I,  $\omega = 0, 10, 25, 50$  and  $100$  s<sup>-1</sup>,  $R_0 = 0.25$  m,  $V/V_0 = 0.5$ . Asterisks mark the bubble complete dissolution.

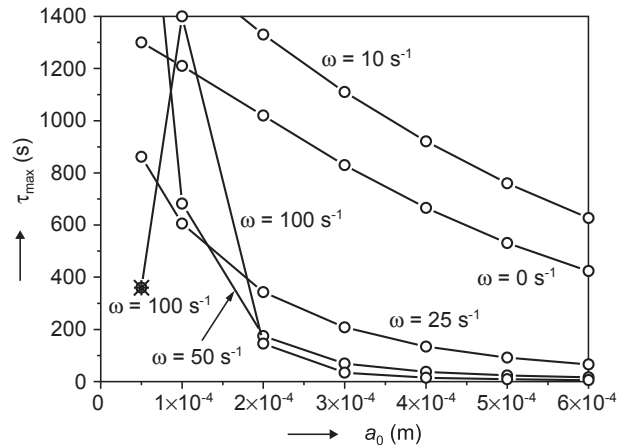


Figure 16. The dependence between  $\tau_{max}$  and  $a_0$ ,  $t = 1400^\circ\text{C}$ ,  $p_{ex} = 1$  bar, case I,  $\omega = 0, 10, 25, 50$  and  $100$  s<sup>-1</sup>,  $R_0 = 0.25$  m,  $V/V_0 = 0.5$ . Asterisks mark the bubble complete dissolution.

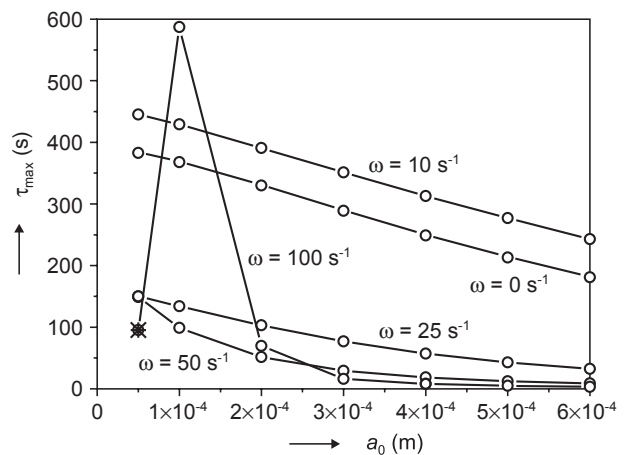


Figure 17. The dependence between  $\tau_{max}$  and  $a_0$ ,  $t = 1500^\circ\text{C}$ ,  $p_{ex} = 1$  bar, case I,  $\omega = 0, 10, 25, 50$  and  $100$  s<sup>-1</sup>,  $R_0 = 0.25$  m,  $V/V_0 = 0.5$ . Asterisks mark the bubble complete dissolution.

indicates high relative efficiency of centrifuging. The average values of the maximum bubble-removal times obtained by centrifuging or by rising and the appropriate values of  $\bar{\tau}_{\max}(\omega)/\bar{\tau}(\omega = 0)$  for the temperatures of 1300-1500°C are summarised in Table 4. The higher the  $\omega$ , the lower the ratio obtained; the lowest relative times, given by the factor  $\bar{\tau}_{\max}(\omega)/\bar{\tau}(\omega = 0)$ , are obtained at the lowest investigated temperature level of 1300°C, the values for case II bubbles at 1300°C are still slightly lower as compared to those of case I (the bubbles in case I contain some fining gas which is diffusing out of bubbles during centrifuging and decreases the bubble radius). The values at 1400 and 1500°C differ only slightly; the application of the highest values of  $\omega$  is restricted by the dissolution of small bubbles, as already mentioned.

The preferred temperature thus lies at 1400-1500°C; the glass containing a fining agent is preferred and the optimal cylinder-angle velocities are 25-40 s<sup>-1</sup>. The application of the lower temperature of 1300°C prefers the usage of a glass without any fining agent. Then, the relative fining times ( $a_0 = 2 \times 10^{-4} \rightarrow 6 \times 10^{-4}$  m) are the lowest, but the absolute values are high for very small bubbles. It is recommended to investigate the possibility of bubble growth prior to centrifuging for case II.

### The impact of pressure

Reduced pressure restricts the bubble dissolution or supports the bubble growth and can accelerate bubble separation using centrifuging. The effect may be apparent and significant only at lower total pressures, i.e. at lower cylinder-angle velocities. Figures 18-20 provide a comparison between  $\tau_{\max}$  obtained from centrifuging and the values resulting from free bubble rising through the corresponding layer of glass under the effect of gravitation ( $\omega = 0$  s<sup>-1</sup> in the figures). These figures show that the absolute values of the maximum bubble-removal times decrease with decreasing pressure, but the ability to compete with free bubble rising through the glass level ( $\omega = 0$  s<sup>-1</sup>) becomes smaller. At 1400°C and a pressure of 0.1 bar, the bubble removal by free rising is faster than centrifuging at the respective  $\omega$  value up to about  $a_0 = 4.5 \times 10^{-4}$  m (see Figure 19), which is roughly valid also for a temperature of 1300°C. The ratios  $\bar{\tau}_{\max}(\omega)/\bar{\tau}(\omega = 0)$ , expressing the relative significance of centrifuging with respect to free bubble rising, are summarised in Tables 5 and 6. The results in both tables provide evidence about the diminishing competitiveness of centrifuging as external pressure decreases. The values of the ratio  $\bar{\tau}_{\max}(\omega)/\bar{\tau}(\omega = 0)$  are lower at

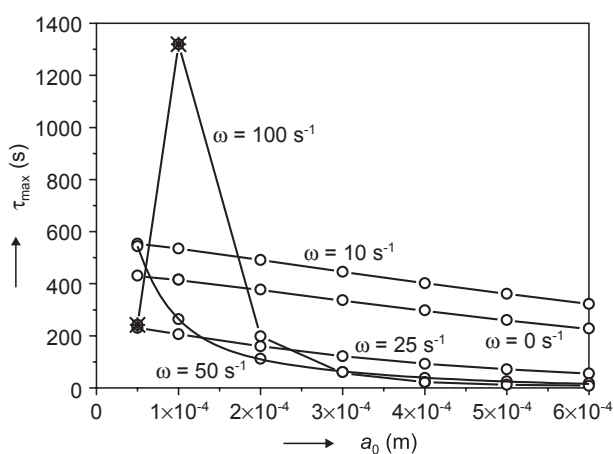


Figure 18. The dependence between  $\tau_{\max}$  and  $a_0$ ,  $t = 1400^\circ\text{C}$ ,  $p_{\text{ex}} = 0.5$  bar, case I,  $\omega = 0, 10, 25, 50$  and  $100$  s<sup>-1</sup>,  $R_0 = 0.25$  m,  $V/V_0 = 0.5$ . Asterisks mark the bubble complete dissolution.

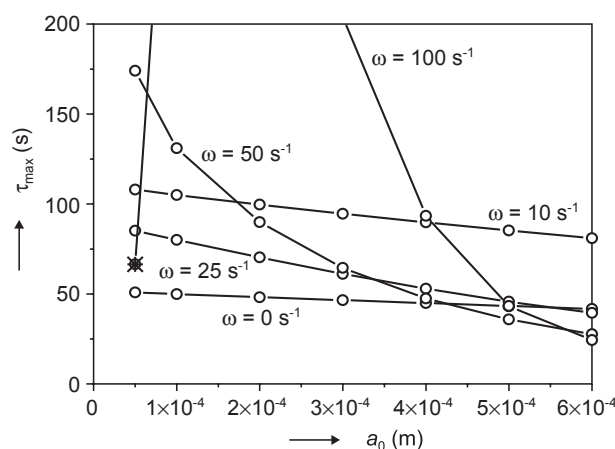


Figure 19. The dependence between  $\tau_{\max}$  and  $a_0$ ,  $t = 1400^\circ\text{C}$ ,  $p_{\text{ex}} = 0.1$  bar, case I,  $\omega = 0, 10, 25, 50$  and  $100$  s<sup>-1</sup>,  $R_0 = 0.25$  m,  $V/V_0 = 0.5$ . Asterisks mark the bubble complete dissolution.

Table 4. The dependence between the ratio  $\bar{\tau}_{\max}(\omega = 0)/\bar{\tau}_{\max}(\omega)$  for  $a_0 = 2\text{-}6 \times 10^{-4}$  m,  $t = 1300, 1400$  and  $1500^\circ\text{C}$ ,  $p_{\text{ex}} = 1$  bar, case I,  $\omega = 0\text{-}100$  s<sup>-1</sup>,  $R_0 = 0.25$  m,  $V/V_0 = 0.5$ . The values in parentheses are valid for case II.

| $\omega$ (s <sup>-1</sup> ) | $\bar{\tau}_{\max}(\omega)/\bar{\tau}_{\max}(\omega = 0)$ |                          |                          | Auxiliary table                 |                          |                          |
|-----------------------------|---|--------------------------|--------------------------|---------------------------------|--------------------------|--------------------------|
|                             | $t = 1300^\circ\text{C}$                                  | $t = 1400^\circ\text{C}$ | $t = 1500^\circ\text{C}$ | $\bar{\tau}_{\max}(\omega)$ (s) |                          |                          |
|                             | $t = 1300^\circ\text{C}$                                  | $t = 1400^\circ\text{C}$ | $t = 1500^\circ\text{C}$ | $t = 1300^\circ\text{C}$        | $t = 1400^\circ\text{C}$ | $t = 1500^\circ\text{C}$ |
| 0                           |   |                          |                          | 4212                            | 694                      | 252                      |
| 10                          | 1.73 (1.72)   | 1.38                     | 1.25                     | 7306                            | 956                      | 315                      |
| 25                          | 0.13 (0.12)   | 0.25                     | 0.25                     | 565                             | 171                      | 62.5                     |
| 50                          | 0.033 (0.027)   | 0.095                    | 0.095                    | 137                             | 65.7                     | 24.0                     |
| 100                         | 0.012 (0.009)   | 0.062                    | 0.081                    | 51.6                            | 43.1                     | 20.3                     |

1300°C, but the differences between the two temperatures disappear at lower pressures (see the values at  $p_{ex} = 0.25$  and 0.1 bar in both tables). The dissolution mechanism has not been completely suppressed, as proved by the asterisks in the figures. At higher  $\omega$ , the dissolution mechanism makes the centrifuging far less advantageous (see maximum of  $\tau_{max}$  for  $\omega = 100$  s<sup>-1</sup> and  $a_0$  around  $2 \times 10^{-4}$  m in Figure 19). In addition, the simultaneous application of both centrifuging and low pressure will certainly involve technical problems. The complete bubble dissolution at higher  $\omega$  is not suppressed because of the relatively high total pressures. The relative effect of reduced pressures diminishes as pressure decreases. The decrease in the absolute values of  $\tau_{max}$  makes the temperatures around 1400°C with pressures

around 0.5 bar and optimal cylinder rotation velocities around 25 s<sup>-1</sup> potentially applicable.

The impact of the cylinder radius and the degree to which the cylinder is filled with glass

An increasing cylinder radius accelerates the bubble centrifuging but is also favourable for the dissolution of small bubbles. A greater cylinder radius thus requires lower cylinder angular velocities to avoid the dissolution process. Various types of glass, characterised by bubbles of certain sizes and compositions are expected to have different optimal cylinder radii. This is different from the ideal case, when the bubbles are completely resistant to dissolution and the fining performance continuously increases with the cylinder radius. The rising amount of glass in the cylinder (the decreasing value of  $r_i$  in Equation (1b)) increases the volume of the fined glass but also supports the bubble dissolution and increases the values of  $\tau_{max}$ . Both in the case of not dissolving and dissolving bubbles, the values of  $\tau_{max}$  tend towards constant values when  $r_i$  becomes smaller (and the amount of glass in the cylinder increased) and on the other side the fining performance of the cylinder goes to zero if  $r_i \rightarrow R_0$  (then, the glass volume in the cylinder is very low).

The changes of both  $R_0$  and  $r_i$  substantially affect the fining capacity of the cylinder, therefore is the fictive cylinder fining performance has been introduced, defined as

$$\dot{V}_{fict} = \frac{V}{\tau_{max}} \quad (8)$$

where the value of  $\tau_{max}$  refers to the value of optimal cylinder-angle velocity.

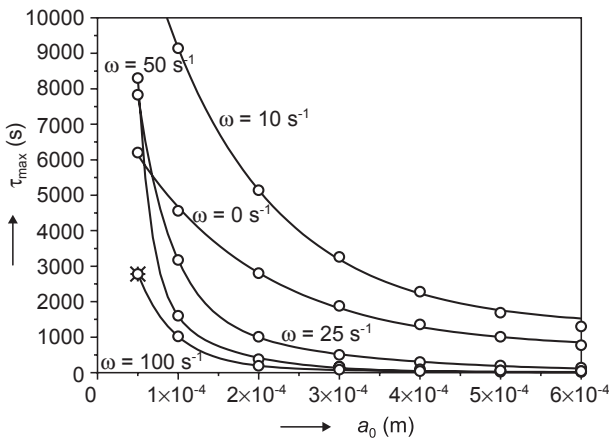


Figure 20. The dependence between  $\tau_{max}$  and  $a_0$ ,  $t = 1300^\circ\text{C}$ ,  $p_{ex} = 0.5$  bar, case I,  $\omega = 0, 10, 25, 50$  and  $100$  s<sup>-1</sup>,  $R_0 = 0.25$  m,  $V/V_0 = 0.5$ . Asterisks mark the bubble complete dissolution.

Table 5. The dependence between the ratio  $\bar{\tau}(\omega = 0)/\tau_{max}(\omega)$  for  $a_0 = 2 \cdot 6 \times 10^{-4}$  m,  $t = 1400^\circ\text{C}$ ,  $p_{ex} = 0.1-1$  bar, case I,  $\omega = 0-100$  s<sup>-1</sup>,  $R_0 = 0.25$  m,  $V/V_0 = 0.5$ .

| $\omega$ (s <sup>-1</sup> ) | $\bar{\tau}_{max}(\omega)/\tau_{max}(\omega = 0)$ |                    |                     |                    | Auxiliary table                |                    |                     |                    |
|-----------------------------|---|--------------------|---------------------|--------------------|--------------------------------|--------------------|---------------------|--------------------|
|                             |   |                    |                     |                    | $\bar{\tau}_{max}(\omega)$ (s) |                    |                     |                    |
|                             | $p_{ex} = 1$ bar                                  | $p_{ex} = 0.5$ bar | $p_{ex} = 0.25$ bar | $p_{ex} = 0.1$ bar | $p_{ex} = 1$ bar               | $p_{ex} = 0.5$ bar | $p_{ex} = 0.25$ bar | $p_{ex} = 0.1$ bar |
| 0                           |   |                    |                     |                    | 694                            | 300                | 119                 | 44.9               |
| 10                          | 1.38  | 1.35               | 1.64                | 2.01               | 956                            | 404                | 195                 | 90.1               |
| 25                          | 0.25  | 0.33               | 0.59                | 1.20               | 171                            | 100                | 70.8                | 53.9               |
| 50                          | 0.095   | 0.17               | 0.41                | 1.18               | 65.7                           | 50.9               | 48.6                | 53.0               |
| 100                         | 0.062   | 0.20               | 0.79                | 4.48               | 43.1                           | 59.4               | 94.4                | 201                |

Table 6. The dependence between the ratio  $\bar{\tau}(\omega = 0)/\tau_{max}(\omega)$  for  $a_0 = 2 \cdot 6 \times 10^{-4}$  m,  $t = 1300^\circ\text{C}$ ,  $p_{ex} = 0.1-1$  bar, case I,  $\omega = 0-100$  s<sup>-1</sup>,  $R_0 = 0.25$  m,  $V/V_0 = 0.5$ .

| $\omega$ (s <sup>-1</sup> ) | $\bar{\tau}_{max}(\omega)/\tau_{max}(\omega = 0)$ |                    |                     |                    | Auxiliary table                |                    |                     |                    |
|-----------------------------|---|--------------------|---------------------|--------------------|--------------------------------|--------------------|---------------------|--------------------|
|                             |   |                    |                     |                    | $\bar{\tau}_{max}(\omega)$ (s) |                    |                     |                    |
|                             | $p_{ex} = 1$ bar                                  | $p_{ex} = 0.5$ bar | $p_{ex} = 0.25$ bar | $p_{ex} = 0.1$ bar | $p_{ex} = 1$ bar               | $p_{ex} = 0.5$ bar | $p_{ex} = 0.25$ bar | $p_{ex} = 0.1$ bar |
| 0                           |   |                    |                     |                    | 4212                           | 1564               | 413                 | 101                |
| 10                          | 1.73  | 1.75               | 2.11                | 2.69               | 7306                           | 2734               | 871                 | 272                |
| 25                          | 0.13  | 0.27               | 0.73                | 2.26               | 565                            | 427                | 303                 | 228                |
| 50                          | 0.033   | 0.093              | 0.40                | 2.25               | 137                            | 145                | 166                 | 227                |
| 100                         | 0.012   | 0.045              | 0.25                | 1.92               | 51.6                           | 70.8               | 105                 | 194                |

The dependences of the fictive cylinder performance on the cylinder radius and the amount to which the cylinder is filled with glass are plotted in Figures 21 and 22. The bubble radii  $a_0 = 5 \times 10^{-5}$  m,  $1 \times 10^{-4}$  m and  $2 \times 10^{-4}$  m have been taken into account as the potential minimum sizes of the bubbles in the cylinder. The values of the optimal cylinder-angle velocities are presented close to the relevant points in both figures. When increasing the cylinder radius or the degree to which it is filled with glass or when decreasing the bubble radius, the shift of the optimal cylinder-angle velocities to lower values is obvious from both figures. The fictive fining performances for smaller bubbles in Figure 21 increase with the cylinder radius, but the very low optimum angular

velocities in both cases will not make a further increase in  $R_0$  possible (the cylinder bottom is completely covered by the glass melt and the effect of centrifuging is very limited). The optimal cylinder radius for bubbles with  $a_0 = 2 \times 10^{-4}$  m is then around  $R_0 = 0.25$  m. Figure 22 shows the growth of  $\dot{V}_{fict}$  with a decreasing cylinder fill for both larger bubbles. The impact of the cylinder filling for the bubble  $a_0 = 5 \times 10^{-5}$  m is not significant. The fictive fining performances incline towards zero as  $V/V_0 \rightarrow 1$  and the optimum filling at  $V/V_0 < 0.5$  may be expected, because  $\dot{V}_{fict} \rightarrow 0$  when  $V/V_0 \rightarrow 0$  ( $r_l \rightarrow R_0$ ). The high fining performances of centrifuging when the very small bubbles are absent are remarkable.

The results show that the optimal cylinder radius as well as the optimal degree to which the cylinder should be filled with glass depends on the type of glass. The undesired dissolution mechanism of the small bubbles at high cylinder radii restricts the optimal cylinder radius to values around 0.5 m, and the decrease in the glass volume inside the cylinder puts the optimum glass fill of the cylinder to values around  $V/V_0 = 0.25$ , low values however limit the throughput. However, the application of small cylinder radii, a low level of cylinder filled with glass and a preliminary removal of the smallest bubbles from the glass shift the optimal cylinder-angle velocities to high values.

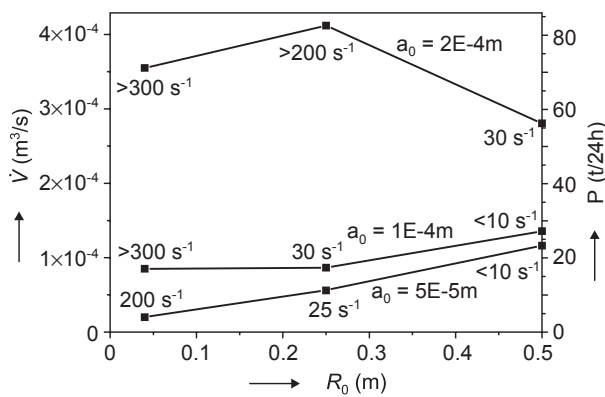


Figure 21. The dependence between the fictive cylinder performance,  $\dot{V}_{fict}$  in  $\text{m}^3\text{s}^{-1}$  (or  $P$  is the amount of refined glass in  $t/\text{day}$ ), and the cylinder radius at the optimal cylinder angular velocity;  $t = 1400^\circ\text{C}$ ,  $p_{ex} = 1$  bar, case I,  $a_0 = 5 \times 10^{-5}$ ;  $1 \times 10^{-4}$ ;  $2 \times 10^{-4}$  m,  $R_0 = 0.04$ ;  $0.25$ ;  $0.5$  m,  $V/V_0 = 0.5$ .  $\omega$  near points are the optimal angular velocities.)

## CONCLUSION

Since glass fining is slow in comparison with other melting processes, the application of the centrifugal force provides a chance to accelerate the whole melting process. However, the gas compressibility and particularly the reaction of the gases with the glass melt make the application of centrifuging relatively complicated. Both rate and quality of centrifugal fining are influenced by several factors, namely temperature, pressure, bubble size and bubble and glass composition, cylinder-rotation velocity, cylinder size and the degree to which it is filled with glass. The crucial role in the process is, however, played by the physical-chemical factors - gas species, number of different gas species and concentrations in the bubbles, their solubility in glass and their diffusion coefficient. The diffusion coefficients of gases were considered constant with pressure, which fact may influence the result accuracy at higher values of  $\omega$  (probably at  $\omega > 50 \text{ s}^{-1}$ ). Nevertheless, the optimum values of the cylinder angular velocities moved below this value. The undesired dissolution mechanism occurs for small bubbles whenever the pressure inside the bubbles increases because of high cylinder angular velocities, cylinder high radius, thick layer of glass in the cylinder or when glass is undersaturated by gases with respect to their partial pressures in bubbles. These factors reduce

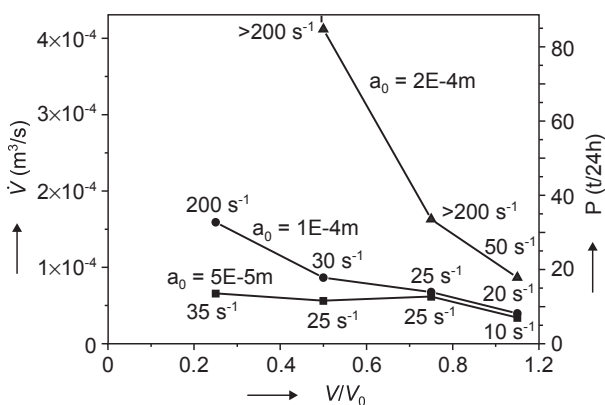


Figure 22. The dependence between the fictive cylinder performance,  $\dot{V}_{fict}$  in  $\text{m}^3\text{s}^{-1}$  (or  $P$  is the amount of refined glass in  $t/\text{day}$ ), and the degree to which the cylinder is filled with glass at the optimal cylinder angular velocity;  $t = 1400^\circ\text{C}$ ,  $p_{ex} = 1$  bar, case I,  $\omega$  near points are the optimal angular velocities,  $a_0 = 5 \times 10^{-5}$ ;  $1 \times 10^{-4}$ ;  $2 \times 10^{-4}$  m,  $R_0 = 0.25$ ,  $V/V_0 = 0.25$ ,  $0.5$ ,  $0.75$ ,  $0.95$ .

the applicable conditions of the centrifugal fining and lead to a search for the optimal cylinder angular velocities for the given set of the remaining conditions. Despite the complicated bubble behaviour aspects mentioned in this paper, relatively small rotating cylinders exhibit high fining performances under the presented proper conditions, and their application is promising. The laboratory verification is needed, consequently, the laboratory furnace with rotating crucible is constructed to verify the modelling results. The modelling of glass centrifugal fining in the continuous regime is desirable.

#### Acknowledgement

*This work is part of the research program MSM 6046137302, 'Preparation and research of functional materials and material technologies using micro- and nanoscopic methods' and Project No. 2A-1TP1/063, 'New glass and ceramic materials and advanced concepts of their preparation and manufacturing', implemented with the financial support of the Ministry of Industry and Trade.*

#### References

1. Beerkens R.: *Analysis of advanced and fast fining process for glass melts*, 7<sup>th</sup> Int. Conf. On Advances in Fusion and Processing of Glass III, Rochester, July 27-31, 2003.
2. Ross C.P.: *Am. Ceram. Soc. Bull.* 83,8 (2004).
3. Kunckle G. E., Welton W. M., Schweninger R. L.: U.S. Patent 4 738 938 (1988).
4. Kloužek J., Němec L., Ullrich J.: *Glastechn. Ber. Glass Sci. Technol.* 73, 329 (2000).
5. Kawaguchi T., Okada M., Ishimura K., Kokubu Y.: *Refining of Glasses under Subatmospheric Pressures-IV*, Proceedings XVIII International Congress on Glass, pp. 39-44, San Francisco, USA, July 5-10, 1998.
6. Bauer R. A.: *Proceedings of the Glass Trend Workshop Melting Concepts for Glass Industry*, Eindhoven, The Netherlands, November 2-3, 2002.
7. Wozniak G., Siekmann J., Sruľies J.: *Flugwiss. Weltraumforsch.* 12, 137 (1998).
8. Merritt R. M., Morton D. S., Subramanian R. S.: *Jour. Coll. Interf. Sci* 155, 200 (1993).
9. Richards R. S., Rough R. R., John S. T.: U.S. Patent 1 360 916 (1972).
10. Katz L. L., Pellett F. G., Rough R. R.: U.S. Patent 1 416 027 (1972).
11. Rough R. R.: U.S. Patent 3 893 836 (1975).
12. Rough R. R. Sr.: U.S. Patent 3 951 635 (1976).
13. Rough R. R.: U.S. Patent 3 992 183 (1976).
14. Němec L., Tonarová V.: *Ceramics-Silikáty* 49, 162 (2005).
15. Tonarová V., Němec L.: *The bubble removal from glass melts in a rotating cylinder*, Proceedings of the 9<sup>th</sup> International Seminar: Mathematical Modeling of Furnace Design and Operation, pp. 43-52, Velké Karlovice, Czech Republic, June 27-29, 2007.
16. Němec L., Tonarová V.: *Ceramics-Silikáty* 50, 216 (2006).

#### TAVENÍ SKEL A JEHO INOVAČNÍ POTENCIÁL: ODSTRAŇOVÁNÍ BUBLIN ZA ÚČINKU ODSTŘEDIVÉ SÍLY

LUBOMÍR NĚMEC, VLADISLAVA TONAROVÁ

*Laboratoř anorganických materiálů,  
Společné pracoviště Ústavu anorganické chemie AVČR, v.v.i.  
a Vysoké školy chemicko-technologické v Praze*

Tato práce se zabývá odstraňováním bublin z rotujícího válce se skelnou taveninou za účinku gravitační a odstředivé síly. Byl vyvinut model chování jednotlivých bublin v tavenině za těchto podmínek a provedena parametrická modelová studie odstraňování bublin v závislosti na teplotě, tlaku, počáteční velikosti a složení bublin, úhlové rychlosti rotace, poloměru rotujícího válce a stupni jeho plnění taveninou. Byla rovněž vyšetřována role obou nalezených mechanismů odstraňování bublin, tj. jejich kompletního rozpuštění v tavenině a separace směrem ke středu válce. Byl nalezen obecný charakter závislosti nejdlejší doby odstranění bublin na úhlové rychlosti rotace, který dovoluje definovat optimální rychlost rotace pro praktické využití. Rovněž byly hodnoceny oba mechanismy odstraňování bublin se závěrem, že rozpouštění bublin je nevýhodný mechanismus a musí být potlačen. Pro chování bublin a efektivnost jejich odstraňování má velký význam jejich interakce s taveninou, tedy fyzikální i chemické rozpustnosti a difúzní koeficienty plynů přítomných v tavenině. Studie byla provedena se záměrem vyhodnotit použití odstředivé síly pro nová uspořádání tavení skel.